Journal of Hydrology: Regional Studies 40 (2022) 101011

Contents lists available at ScienceDirect

Journal of Hydrology: Regional Studies

journal homepage: www.elsevier.com/locate/ejrh

Investigating groundwater recharge potential of Notwane catchment in Botswana using geophysical and geospatial tools

Otlaadisa Tafila[a,*], Rubeni T. Ranganai[a], Ditiro B. Moalafhi[b], Kealeboga K. Moreri[c], Joyce G. Maphanyane[b]

[a] *Department of Physics, University of Botswana, Private Bag, UB00704 Gaborone, Botswana*
[b] *Department of Environmental Science, University of Botswana, Private Bag, UB00704 Gaborone, Botswana*
[c] *Department of Civil Engineering, University of Botswana, Private Bag, UB0061 Gaborone, Botswana*

A R T I C L E I N F O

Keywords:
Apparent susceptibility
Euler deconvolution solution
Groundwater recharge potential
Notwane Catchment Area (NCA)
Remote sensing
Geospatial tools

A B S T R A C T

Study region: This study is conducted over the Notwane Catchment Area (NCA) in Southeastern Botswana using geospatial and geophysical tools.
Study focus: Geospatial and geophysical tools, which provide spatial information for both the surface and subsurface have been widely used in groundwater exploration because of their capability in detecting physical properties that are related to groundwater phenomena. In this research, relevant remotely sensed data including aeromagnetic data and satellite images were used to identify potential groundwater recharge zones within the NCA as a contribution towards improved water resources management amid the changing climate. The multi-disciplinary approach used could offer a more reliable way to identify potential recharge zones, particularly in semi-arid hard rock terrains.
New hydrological insights for the region: Assessment of groundwater recharge potential looking at remotely sensed data revealed that built-up areas expanded significantly between 2009 and 2019 with implications for run-off and flooding. Through aeromagnetic data interpretation of Euler deconvolution solutions and apparent susceptibility computations, weathered zones and geologic lineaments, mainly dykes and faults, indicating areas with increased secondary porosity were identified. Consequently, the groundwater recharge optimization model was used to determine areas with higher recharge potential which lie on the central part of the NCA, northeastern margin and the southernmost part bounded by topographical relief of hills with thick vegetation. These areas are characterized by approximately 200 m depth of weathering and predominantly east-west structural features.

1. Introduction

Groundwater recharge has been ordinarily through natural means and with the rise in discharge through boreholes and water wells, there has been increased use of artificial recharge techniques crafted to augment groundwater recharge. These techniques involve the development of models that seek to identify potential areas where groundwater recharge can be considered to harness surface runoffs during the short and often unpredictable rainy seasons. Harvested surface runoff can be directed to potential recharge zones and if need

* Correspondence to: University of Botswana, Department of Physics, Plot 4775 Notwane Rd, UB 0022, Gaborone, Botswana.
E-mail address: tafilao@ub.ac.bw (O. Tafila).

https://doi.org/10.1016/j.ejrh.2022.101011
Received 25 October 2021; Received in revised form 11 January 2022; Accepted 24 January 2022
Available online 1 February 2022
2214-5818/

be, other alternatives of artificial groundwater recharge like pumping wells can benefit from the temporary stored rainwater. It is expected that artificial recharge will become a very critical component of water resources management and planning as population growth and increased per capita consumption into the future requires water (Kumari and Krishna, 2013) Artificial recharge of groundwater is a practical option that makes the best use of unused water resources in replenishing aquifers (Hammouri et al., 2014). This will undoubtedly relieve the increased pressure on groundwater resources which is often anchored on more technological developments in groundwater exploration which increases the rate of discharge more than the resource can recover. However, if not well planned, structures made along drainage system to harvest surface runoff and storm water do not benefit downstream water sources as most of the water is arrested until local areas are saturated to the detriment of downstream users. As highlighted by Chanda et al.

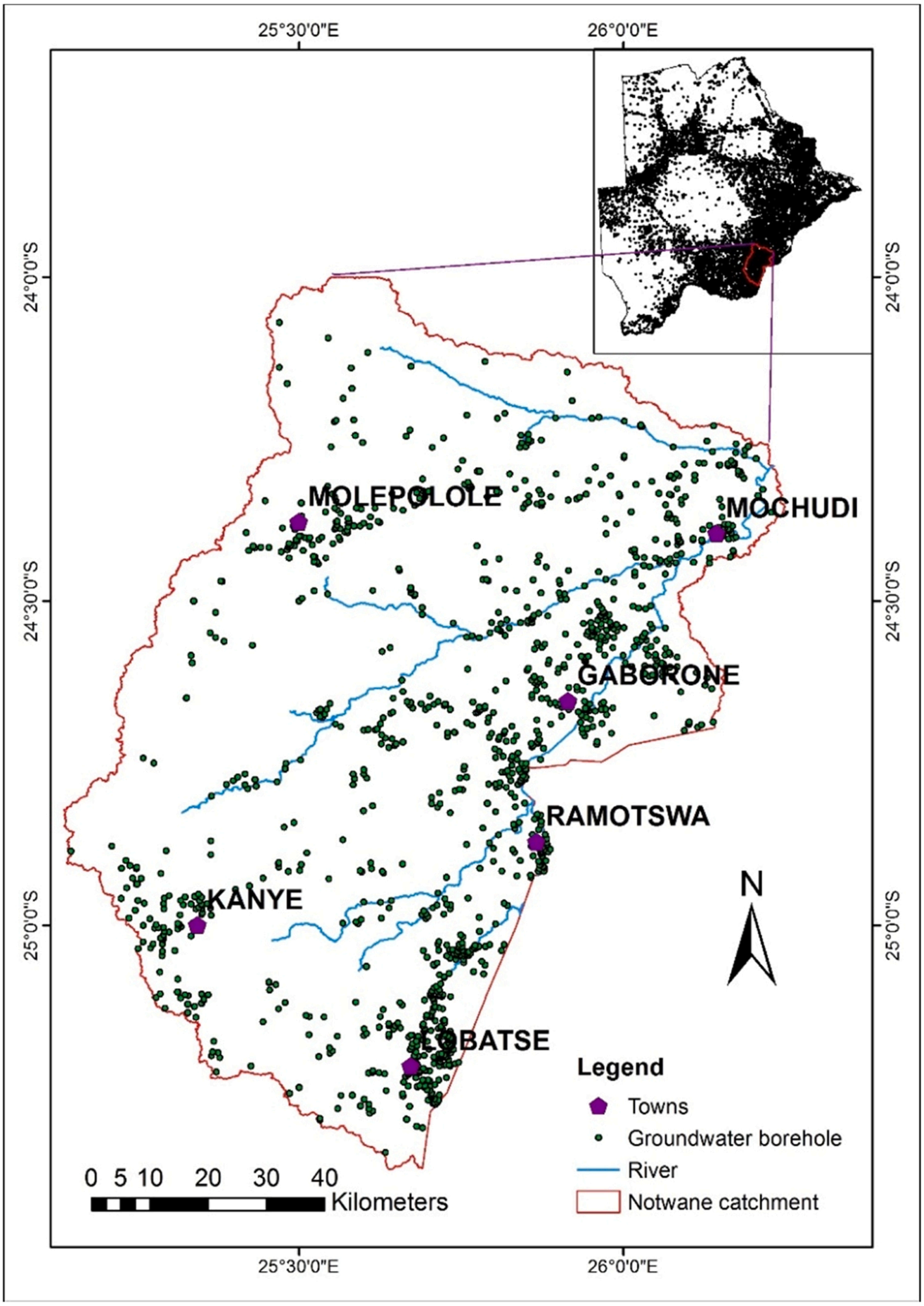

Fig. 1. Notwane catchment showing groundwater boreholes distribution densely populated in the eastern part of Botswana following major population centres, including the capital city of Gaborone.

(2018), this scenario occurred in the Notwane catchment where debates pointed to small upstream dams as partly responsible for the Gaborone dam's failure by late 2015 until cyclone *Dineo*'s downpours filled the dam to full capacity in the 2016/2017 rain season.

The Notwane catchment area (NCA), which is the study area, covers about 9260 km^2 and hosts the largest population cluster in Botswana that has the highest demand of portable water and a significant number of groundwater boreholes (Fig. 1). In the current setting, the greater Gaborone area usually experiences flooding which results in storm water being viewed as nuisance because of its urbanizing landscape. Challenges of lack of management of storm water and excessive abstraction of groundwater often lead to impairment of fragile aquifers. This research therefore aims to identify suitable sites within the NCA where excess runoff can be used to restore drawn groundwater to lessen aquifer impairment. Artificial recharge of groundwater as a practical option makes best use of unused water resources in replenishing aquifers (Hammouri et al., 2014).

The conceptual framework guiding this research is aimed at maintaining sustainable groundwater resources through monitoring and data collection of groundwater levels; determining environmental groundwater depth; implementing groundwater resources management through recharge and the feedback and adjustment processes. The following diagram in Fig. 2 shows an adopted and modified conceptual framework of environmental groundwater depth and sustainable groundwater resources management from Huang et al. (2019) and da Costa et al. (2019) respectively. The induvial frameworks were adapted and incorporated in this study because of the interlinkages of the spatially distributed recharge processes and groundwater levels which are significantly affected by the ever-increasing number of boreholes drilled.

Borehole monitoring stations within the catchment provide temporal data of groundwater water levels. Tafila (2020) analyzed for visible trends where recharge, discharge and balanced groundwater depths against rainfall amounts were inferred for rising, declining and sustainable use of groundwater rates respectively. The environmental groundwater depth phase is established from groundwater level response obtained from monitoring data. The pressure exerted on the aquifer determines if the water table is lowered by excessive water abstraction or rising due to natural or artificial recharge where rainfall is the source of groundwater recharge. The implementation of water resources management step informs actions and policies to be implemented when abstracting groundwater whilst achieving sustainable use of the resource. The human population, groundwater boreholes and activities in the area determine the amount of water used. Balancing between the rate of discharge and recharge to optimize resource use is for sustainability and the ultimate aim of water resources management. In this regard, employing groundwater recharge techniques through the use of GIS and spatial analysis in identifying potential recharge zones is critical to the maintenance of optimum groundwater levels. The major source of groundwater recharge is precipitation through natural recharge and induced recharge techniques which are accurately positioned in a zoned map of potential recharge. Different thematic layers overlaid in a GIS environment will determine suitability of individual sites derived from geospatial data. The final phase in the multi-step framework of maintaining sustainable groundwater resources ensures that the target of sustainable groundwater resources is achieved through adjustments in recharge and abstraction rates.

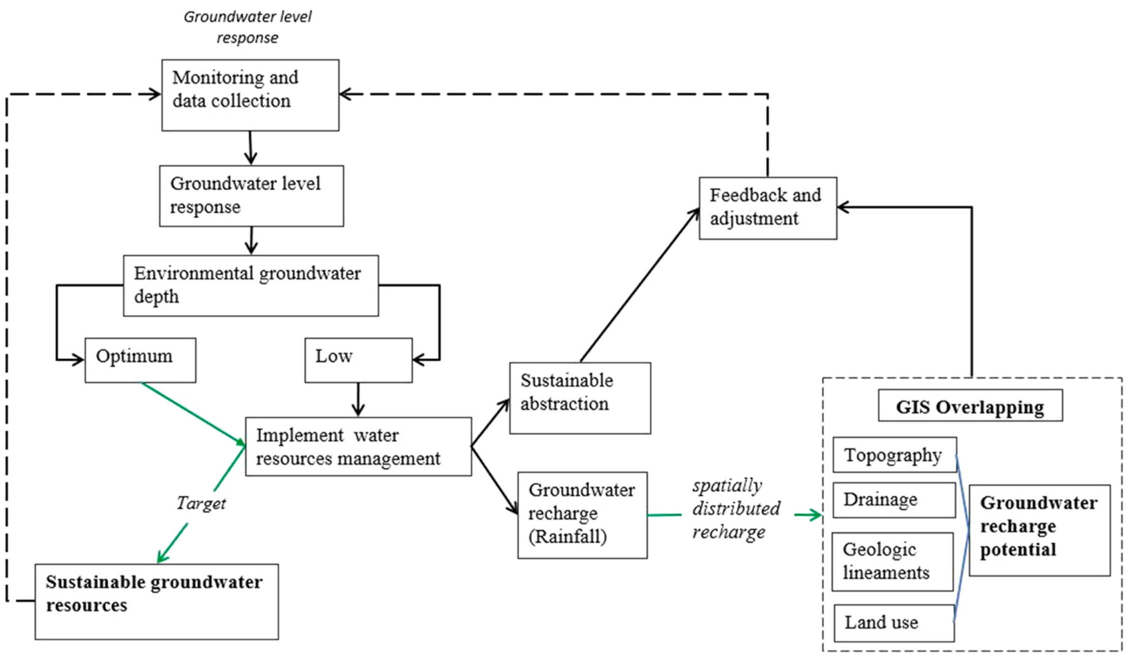

Fig. 2. Sustainable groundwater management 'hybrid' framework adopted from Huang et al. (2019) and da Costa et al. (2019).

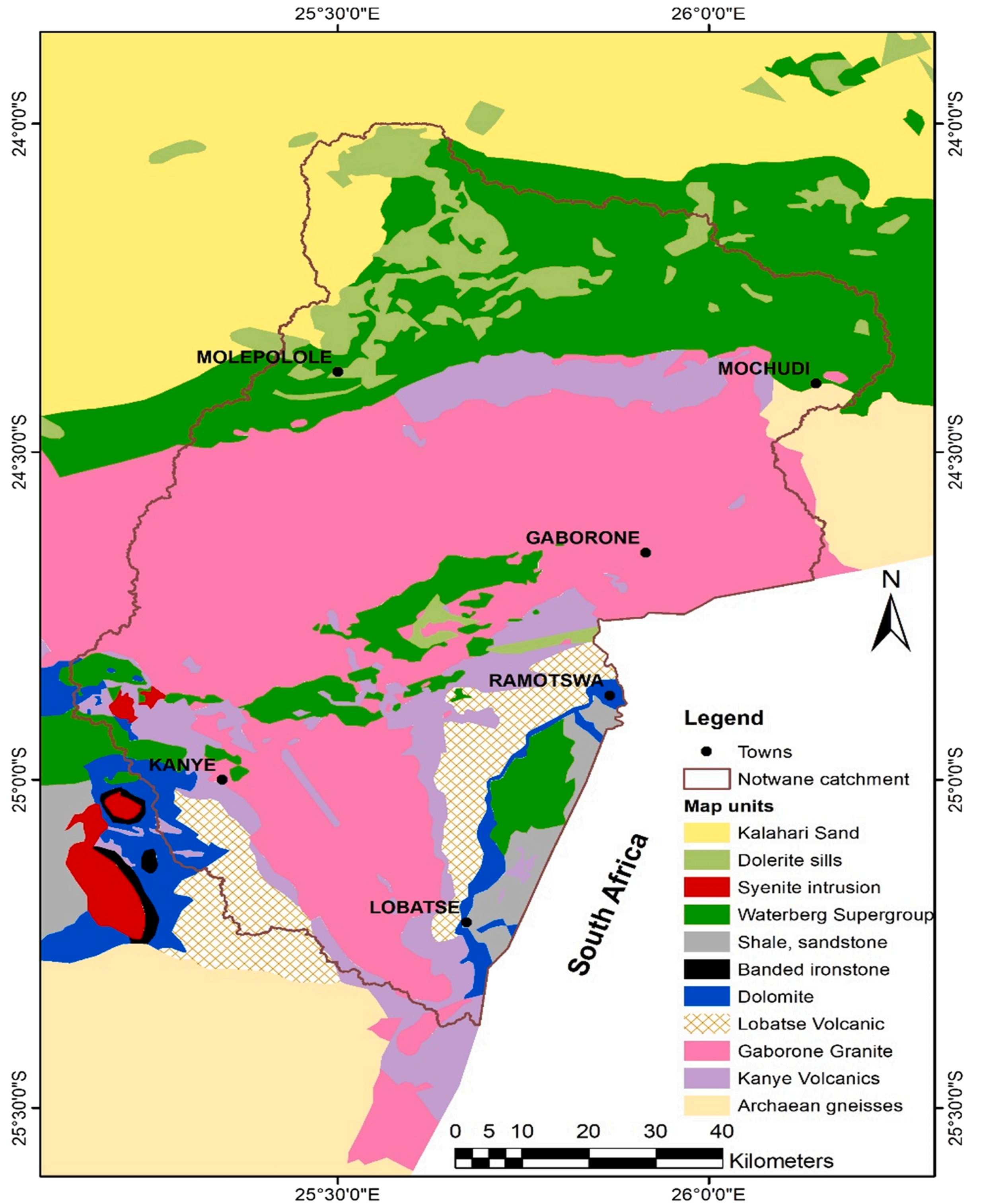

Fig. 3. Simplified regional geology map of the study area.
Modified from Gieske (1992).

2. Geology and hydrophysical setting of the NCA

The NCA is mostly covered by the Gaborone granite and the Waterberg supergroup with spatial extents indicated on the geology map (Fig. 3). Kanye volcanics represents a series of highest topographic relief zones of the area. The study area has highest elevations on the southwestern side reaching 1496 m while the surface discharge point is to the northeastern side and has the lowest elevation of about 918 m. The catchment outlet at the discharge point is a convergence of river systems passing through the city of Gaborone and its immediate environments. This geographical region is characterized by highly variable and scarce rainfall. Summer rainfall over the area comes between October and March averaging around 500 mm per annum. Annual evapotranspiration, which exceeds annual rainfall, peaks between the months of January and April during the rainy season (Moalafhi et al., 2018). Temperatures can reach maximums of 40 ^{0}C during summer, with winter temperatures going as low as 7 ^{0}C.

Availability of groundwater in the area's hard rock terrains is limited with occurrences only confined to fractured and weathered zones which provide secondary porosity. Dijon (1984) observed that Precambrian rocks have fracture zones associated with faults and weathering along the strike to form deep basin as cited by Botha and Van Rooy (2001). These weathered zones correspond with low topographic elevations and drainage systems. The topographic lows subsequently serve as water recharge zones because surface water that has accumulated in the depressions percolate into the subsurface with the aid of gravity and suitable ground transmissivity. Chuma et al. (2020) have also observed that geological setting greatly influences existence of crystalline basement aquifers in a similar study conducted in Bulawayo, Zimbabwe.

3. Methodology and data

An integrated approach of using geospatial and geophysical techniques in this study is that satellite imagery interpreted with the respective subsurface physical properties from geophysical data offers a unique perspective of surface and groundwater availability and interactions. Satellite images are currently being used to identify ground features that are presumed to be direct and indirect indicators of groundwater potential (Rashid et al., 2012) while geophysical methods are used to remotely gather the subsurface properties of the underlying geology (Roy, 2014). Aeromagnetic data was processed and interpreted with the goal of mapping geological structures and weathered zones within the Notwane catchment. On the other end, satellite images were used to assess the surface for Land cover/ Land use as well as river networks and drainage system in the catchment.

3.1. Aeromagnetic data processing and Interpretation

The use of certain geophysical methods is determined by the objective of the research. The investigation of the subsurface is made relevant to geological structures that aid in the capacity to store and recharge the groundwater sources with surface runoff. Ideally, lineaments including dykes and faults which form secondary porosity to store water and are conduits to groundwater flow are best investigated from aeromagnetic data processing as discussed below.

3.2. Euler deconvolution and apparent susceptibility

Aeromagnetic data is the data obtained remotely from aircraft and bears the magnetic strength of the rocks over the survey area. The total field, as discussed by Dentith and Mudge (2014), is usually referred to as the total magnetic intensity (TMI) which is usually the resultant of a vector sum of the vertical and the two horizontal components (x, y, z) of the field and measured in nanoTesla.

An IGRF (International Geomagnetic Reference Field) corrected archive aeromagnetic data used for this research was obtained from the Botswana Geoscience Institute. This data was acquired between 1986 by Geosurvey International GmbH using Scintrex Cesium vapour magnetometer of 0.01 nT sensitivity. Flight lines were 1 km apart at mean terrain clearance of 150 m. Data preparation for this exercise included windowing aeromagnetic grid sufficiently covering the study area from the recompiled nationwide magnetic data. The data bears an enhanced 50 m resolution magnetic grids released by the then Department of Geological Survey in 2012 following a nationwide Tie Line Survey of airborne magnetics in 2010–2011 (Reford et al., 2013).

The interpretation of the aeromagnetic data was done with the aim of determining the orientation and spatial extent of lineaments found in the NCA because they play a major role in the flow of groundwater. The initial process of analyzing aeromagnetic data included the reduction to pole which was done in order to reduce the effect of magnetic inclination which has an advantage of improving interpretation of the map by centering the anomalies directly above their sources. Detail-enhancement filters were also applied to the aeromagnetic data to emphasize the edges of linear features in the TMI grid and outline zones of weathering from calculating magnetic susceptibility. Depth of weathering is important for water percolation.

The output of processing aeromagnetic data is the production of lineament density map which was used to validate the structural lineaments obtained from processing satellite images of the area. Takorabt et al. (2018) have also confirmed the presence of structural lineaments of Landsat 7 ETM+ satellite images using geophysical results and geological map.

Geological lineaments of shallower to a few hundred meters of depth are of importance to groundwater dynamics which sustains the lives of humans and vegetation by providing fresh water. The depth to sources and locations of magnetic sources where lineaments were derived from anomaly gradients were computed using the Euler deconvolution technique.

The Euler's equation adapted by Reid et al. (1990) is given by

$$(x - x_o)\frac{\partial f}{\partial x} + (y - y_o)\frac{\partial f}{\partial y} + (z - z_o)\frac{\partial f}{\partial z} = N(B - f) \tag{1}$$

which represents the strength (f) of a potential field, in this case magnetic, at a point x, y, z in space due to a source located at x_o, y_o, z_o, in terms of the first order derivatives ($\partial f/\partial x$), ($\partial f/\partial y$) and ($\partial f/\partial z$); regional background component (B) and the structural index (N).

The structural index that was used in this objective was one (1) which is targeted at the rate at which the field (f) falls off with distance for approximately linear features such as faults, dykes and sills (Reid et al. (1990), which encourage secondary porosity in hard rock terrains (Roy, 2014). Several indices have been derived for other source types as discussed by Dentith and Mudge (2014). A 50 m square window was used, as the depth estimation procedure relies on the field curvature within the data window used, and the minimum depths returned are about the same as the grid interval while the maximum depths are about twice the window size (Reid et al., 1990). Solutions with a depth tolerance greater than 5% were discarded.

In addition to aeromagnetic data processing, apparent susceptibility k calculation yields measurable estimates of the relationship between magnetic flux density $\boldsymbol{B}$ and magnetizing force $\boldsymbol{H}$**.** This relationship is given by

$$B = kH \tag{2}$$

Apparent susceptibility is an inversion technique that was used to convert the magnetic field strength into an apparent physical property map by applying a compound filter. The physical property map approximates true susceptibilities and gives an indication of the local geology (Silva and Hohmann, 1984). The susceptibility filter comprises of reduction to the pole, downward continuation to the source depth, correction of the geometric effect of a vertical square ended prism and division by the total magnetic field to yield susceptibility (Grant, 1973). The apparent susceptibility of the prism as presented by Yunsheng et al. (1985) is given by the relation:

$$\mathrm{T(u, v) = 2\pi ToM(u, v)H(u, v)S(u, v)KjDj(x, y; u, v)} \tag{3}$$

where T_o is the Earth's magnetic field intensity; M(u,v), H(u,v), S(u,v), D_j(x,y; u,v) are magnetization, depth, size, displacement factors respectively; K being the susceptibility; u,v representing wavenumbers in x,y direction and j denoting the prism index in a grid of n prisms. The size and magnetization factors are the same for all prisms while reduction to the pole and downward continuation removes the displacement and depth factors, respectively.

Rocks highly concentrated with ferro- and/or ferrimagnetic minerals tend to have high susceptibilities; acidic igneous and metamorphic rocks having average to low susceptibilities while sedimentary rocks have generally low susceptibilities (Reynolds, 2011). Apparent susceptibility of the aeromagnetic grid of the study area was calculated to determine the degree of geologic alteration in the study area which is also affected by groundwater presence. Ranganai and Ebinger (2008) have acknowledged the use of apparent susceptibility maps in identifying areas with potential for deep weathering, alteration zones or thick permeable regolith.

3.3. Satellite imagery (remote sensing)

The significance of satellite data is that they provide invaluable information on the surface properties of the ground which affects the hydrological process of the area. Enhancement of satellite imagery comes handy when interpreted for lineament mapping, Land use/ Land cover and DEMs (Digital Elevation Models) for extracting drainage patterns of an area.

3.4. Land use / land cover mapping

Land covers in an area can create an impervious layer which alters the hydrology of the area causing flooding or allowing surface waters to percolate into the subsurface dependent on the transmissivity of the ground. The infiltration rate which is also affected by different land covers controls surface water flow and with impervious surfaces, excess water begins to accumulate as surface storage in small depressions governed by surface topography which could potentially recharge groundwater sources by percolation or lost through evaporation. The significance of land cover mapping helped in demarcating the general areas which are semi-impervious like built up areas and portions that bear the natural landscape of the area.

The land cover classification of the study area was carried out through supervised image classification of 2009 Landsat 7 ETM+ and 2019 Landsat 8 OLI/ TIRS images covering the study area for the rows and paths indicated in Table 1. These satellite images were chosen considering the spatial resolution of 30 m which improved the output of land cover classes with a higher resolution. The changes in land cover between 2009 and 2019 were expected to be significant in creating imperviousness and/or altering runoff generation with implications for ground water recharge.

A total of 6 major land cover land use classes were identified in the study area by virtual interpretation which were considered for image classification. A standard false colour of 5, 4, 3 representing blue, green and red respectively for Landsat 8 OLI/ TIRS and 4, 3, 2

Table 1
Selection of images for land cover mapping.

Year (Month)	Landsat Mission	Spatial resolution	Rows and Paths
2009 (March)	Landsat 7 ETM+	30 m x 30 m	Path:172
2019 (March)	Landsat 8 OLI/ TIRS	30 m x 30 m	Row:077

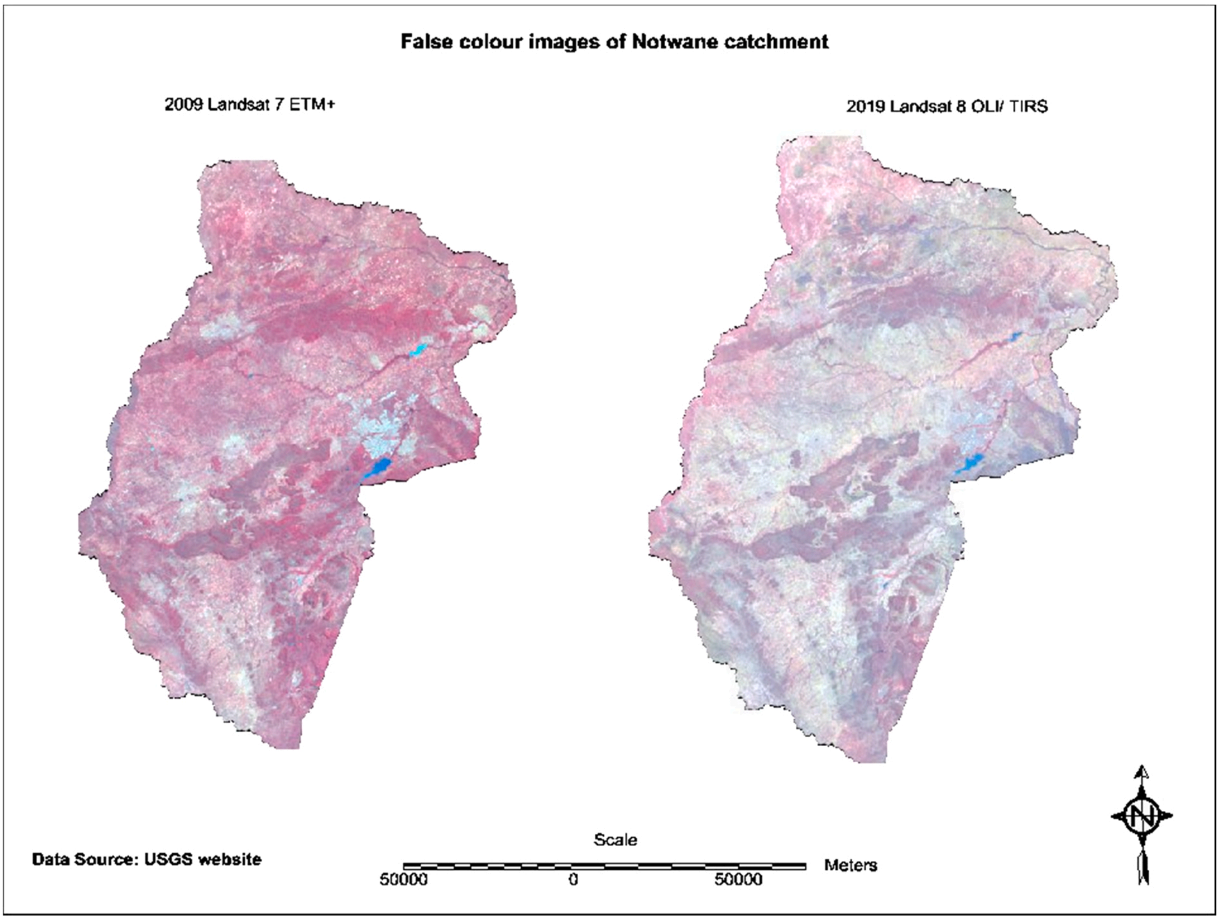

Fig. 4. Standard false colour Landsat 7 and 8 images (2009 and 2019 respectively) of the NCA.

Table 2
Major land cover types identified through conceptualizing the extended legend for land cover classes in Fig. 4.

Land cover/ Land use	Description
Water body	An area that accumulates surface water such as depressions on the ground and man-made structures including dams and reservoirs.
Built-up	Land characterized by human settlement with high population density and activities of built environment and infrastructures.
Sparse vegetation	Land with rare patches of trees with a mixture of grass and sparsely distributed shrubs.
Thick hilly vegetation	Land cover with relief topography higher than surrounding areas dominated by thick shrubs and trees.
Dense/ Woody vegetation	Area of land with densely populated trees and riparian vegetation with similar characteristics of tall trees and less grass cover.
Arable/ Bare land	Land used for crop production including fallow land, cultivated land and debushed or cleared land.

for Landsat 7 ETM+ enhanced the images for assessing the classes of land covers in Fig. 4. These classes are described in Table 2.

A ground-truthing follow-up was carried out at designated points generated through systematic sampling to ensure that all land cover classes are checked to evaluate the performance of the classification algorithm. This process is referred to as accuracy assessment. Congalton and Green (2008) outlined the importance of knowing the accuracy of a map produced as effective decisions about the extent and distribution of resources lies on accurate maps or at least maps of known accuracy.

3.5. Lineament mapping

Lineaments are classified as either edges or lines on a digital grey scale image (Farahbakhsh et al., 2018). The exercise of lineament mapping is a systematic process that involves satellite image processing techniques to extract linear features which are surface expressions of the local geology of an area.

The main advantage of lineament detection to this study is that geological lineaments (dykes, faults, fractures, surface discontinuities, cleavages, river reaches) are an integral part which largely controls groundwater flow. However, Yeh et al. (2016) noted that this approach of lineament detection in satellite imagery is capable of detecting non geologic features like paths, roads that can be misinterpreted from satellite images and subsequently causing errors in the analysis of lineaments hence the need for validation using geophysical methods which have the advantage to remotely image the subsurface. Zeil et al. (1991) also emphasized the need for an integrated approach using aeromagnetic data as prevalent cover can considerably conceal detection of lineaments from satellite imagery. Ranganai and Ebinger (2008) further add that aeromagnetic data investigates deeper lineaments than Remote Sensing. River reaches were detected through a series of networking lineaments following riparian vegetation and low elevations for drainage characterization. Non geologic lineaments helped in demarcating built-up areas from other land classes which are characteristics possessed by this class over other land covers.

3.6. DEM and drainage networks

Digital terrain model is a three dimensional surface of the terrain that is packed with digital information where a variety of hydrological and terrain characteristics of an area can be extracted (Saraf et al., 2004). Digital terrain modelling was performed for this research to derive the slope, aspect, flow accumulation and stream networks within the Notwane catchment. These terrain properties provide invaluable information about the study area where the core objective is the understanding of water flow dynamics from the surface into the subsurface. Saraf et al. (2004) further elaborates on the derivatives of DEM not just being a spatial distribution of elevation with reference to an arbitrary datum but other variables like groundwater levels, chemical qualities of water can be also represented. The DEM for the area was obtained from the Shuttle Radar Topography Mission (SRTM).

3.7. Groundwater recharge optimization – GIS (Weighted overlay analysis)

The data collected for the study area and ancillary data from document study was integrated in a GIS environment to produce a groundwater potential recharge site map for the area. This integration draws optimum synergy of geophysical data and other remotely sensed data. The different thematic maps derived from the discussed methodologies were assigned relative weights and rankings according to their suitability in aiding groundwater recharge using Analytic Hierarchy Process (AHP) approach. The thematic maps for the area constituted spatial data consisting of lineament density map, slope, elevation, land use/ land cover, drainage network (Flow accumulation), apparent magnetic susceptibility and soil types.

Weighting criteria developed by Saaty and Vargas (2012) for assigning weights to the variables used in this process is shown in Table 3. This weighting criteria simply ranks a variable against another according to the objective and desired output in which case for this study, variables were compared on their importance to aiding groundwater recharge. Saaty and Vargas (2012)'s pairwise comparison scale was used to determine the relevance of the variables (e.g., lineaments in first row) in Table 4 to other variables (column 2–8) to determine the weight of each variable in the last column. In this example, when lineaments are compared to lineaments, the judgment yields an equally important result but when compared to land cover, lineaments are extremely important. The overall weight assigned to each variable was dependent on individual comparison of lineaments to the other six variables. This step was repeated for the other 6 variables. The steps involved in calculating the weights entailed summing up the columns to generate a scaled influence measure which was later used to normalize the matrix as discussed by Mu and Pereyra-Rojas (2017). Occurrence of inconsistencies in judgments is resolved in the AHP process and it provides means of improving consistency (Saaty and Vargas, 2012).

The analytic hierarchy process was used to analyze data for groundwater recharge potential over the catchment in which the variables were scaled and weighted based on literature and best judgment (Maxwell, 2018). Soil types and land cover classes which were part of the inputs in modelling groundwater optimization datasets were assigned discrete values according to their relative influence on groundwater recharge since their data is not continuous. For soil types, these scales were based on Field Soil Moisture Capacity (FSMC) of different soils within the study area which correspond to their clay content whereas land cover was based on the level of permeability of different classes. Other data sets which were continuous were scaled from 0 to 1 indicating low to high respectively and this included elevation, slope, apparent susceptibility, lineament density and flow accumulation in which the last two were converted to continuous data by calculating the Euclidean distance from the features. These variables affect groundwater recharge and discharge. The drainage patterns and amount of rainfall within the study area are also critical to groundwater recharge.

Table 3
Saaty's pairwise comparison scale.

Verbal judgment	Numeric value
Extremely important	9
	8
Very strongly more important	7
	6
Strongly more important	5
	4
Moderately more important	3
	2
Equally important	1

Table 4
Weights applied to the AHP model for groundwater recharge potential.

	Lineaments	Apparent susceptibility	Soil	Slope	Elevation	Land cover	Flow accumulation	Weight (%)
Lineaments	1	3	4	6	8	9	6	37.93
Apparent susceptibility	1/3	1	4	5	6	8	5	24.79
Soil	1/4	1/4	1	5	7	7	2	15.80
Slope	1/6	1/5	1/5	1	5	2	1	6.90
Elevation	1/8	1/6	1/7	1/5	1	4	2	5.37
Land cover	1/9	1/8	1/7	1/2	1/4	1	4	4.99
Flow accumulation	1/6	1/5	1/2	1	1/2	1/4	1	4.22
Sum	2.15	4.94	9.99	18.70	27.75	31.25	21.00	100.00

4. Results and discussions

4.1. Euler deconvolution and magnetic susceptibility

Processing of archive aeromagnetic data with fitting algorithms discussed in the methodology chapter to draw inferences on major regional features of groundwater importance yielded lineament and standard Euler deconvolution solution maps (Figs. 5 and 6 respectively). Predominant structures and their trends show that the area has geologic lineaments with varying orientations on areas which were gridded during data collection. Lineaments present secondary porosity which controls ground water flow by either creating barriers (dykes) or path (faults).

Most of the lineaments drawn from Standard Euler solutions are in shallow depth range of 0–100 m (Fig. 7) which play a significant role on groundwater flow that is easily accessible for abstraction. Ranganai and Ebinger (2008) also acknowledged the same fact about lineaments bearing considerable depth likely to be open groundwater conduits. Hard rock terrains as is the case with the local geology (fresh granites) within NCA presents limited groundwater availability as compared to weathered and fractured subsurface.

The vertical derivative map (Fig. 5) shows enhanced lineaments and edges of magnetic bodies. The faded portion on the greater Gaborone area is a result of no data recorded in the area and covered by interpolated values at a larger cell size. The cell size for the grids used here was 50 m and a projected coordinate system of UTM zone 35. Part of the muted area shown in the map in Fig. 5 were not surveyed due to restricted activities and security reasons for military airbase which lies on the western part of the study area.

The Standard Euler solutions plotted here were categorized on depth ranges of 0–100, 100–200 and depths of more than 200 m. A 10% tolerance of solutions was set in order to generate more reliable solutions which were later filtered based on dXY, X_offset and Y_offset which yielded fewer solutions.

Lineaments in the Notwane have varying orientations, length as well as depths. Majority of the lineaments are shallower whereas deeper ones show similar orientation and slightly varying lengths at the same ground locations. The area surrounding the greater Gaborone do not show lineaments as there was no data for computing the Euler deconvolution in the area.

The apparent susceptibility map shows distinct apparent susceptibilities where areas at higher elevations (Fig. 10 a) corresponds with high apparent susceptibilities. The central part of the catchment has average apparent susceptibilities compared to elevated areas and those exhibiting lower apparent susceptibilities.

Magnetic susceptibilities have a geological significance on the degree of alteration of rocks due to groundwater presence. There is higher apparent susceptibility range in the general Notwane catchment which provides a varied option to suitable sites for groundwater recharge based on the apparent susceptibilities calculated. Southern parts of the catchment and an area near Mochudi have high apparent susceptibilities which could be inferred to be strongly magnetized rocks whereas other areas have low apparent susceptibilities of − 0.00092 that could be associated with deeply weathered, oxidized igneous and metamorphic rocks and rarely non-magnetized sediments since the Notwane area overlays a crystalline basement. The advantage of having both these extreme susceptibilities is that weaker apparent susceptibilities present a fitting environment for groundwater recharge while formations with high apparent susceptibilities would bound and control groundwater flow from escaping the point of recharge. Other areas fall within the average spectrum of apparent susceptibility. The greater Gaborone area shows noisy streaks on this spectrum which is a result of data unavailability.

4.2. Satellite image processing

4.2.1. Land cover

The map in Fig. 9 shows six major classes of Land use/ Land cover found in the study area for two years, 2009 & 2019. The change in land cover between this period is summarized in Table 5 which shows gains and losses of different classes. Error matrix and accuracy assessment results of 2019 land cover map are also shown in succeeding Table 6.

Precipitation is the source of water that feeds both surface and groundwater sources where landcover is the primary filter of surface water that seeps and flow through the drainage system of the area. The six major landcovers identified in the area have different impacts on the dynamics of percolation. The overall accuracy assessment of the 2019 image was 75.5%.

This area is mostly covered in vegetation of varying densities and the natural landscape has been preserved for more than 96% of the total Notwane area as of 2019. Thick hilly vegetation which is indicative of abrupt topographic change mostly influences the surface flow of runoff or barrier to storm water or floods. This area covers about 15% of the area and resembles geologic structures that

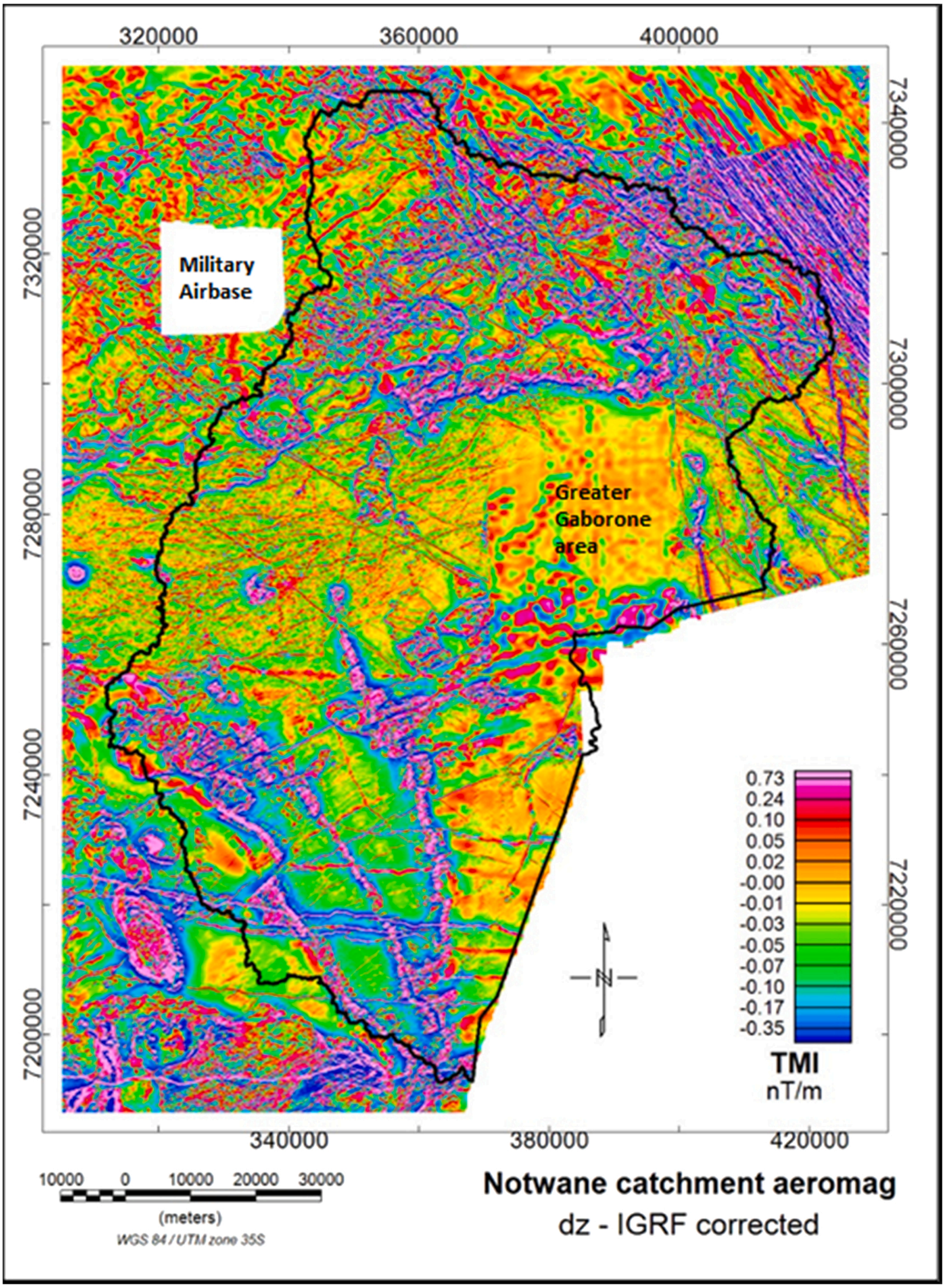

Fig. 5. First order derivative in z direction calculated from reduced-to-pole grid. Preliminary processing of aeromagnetic data using a 'reduction to pole' filter was applied to the IGRF corrected aeromagnetic grid which yielded an input to vertical derivative calculation shown in the image above.

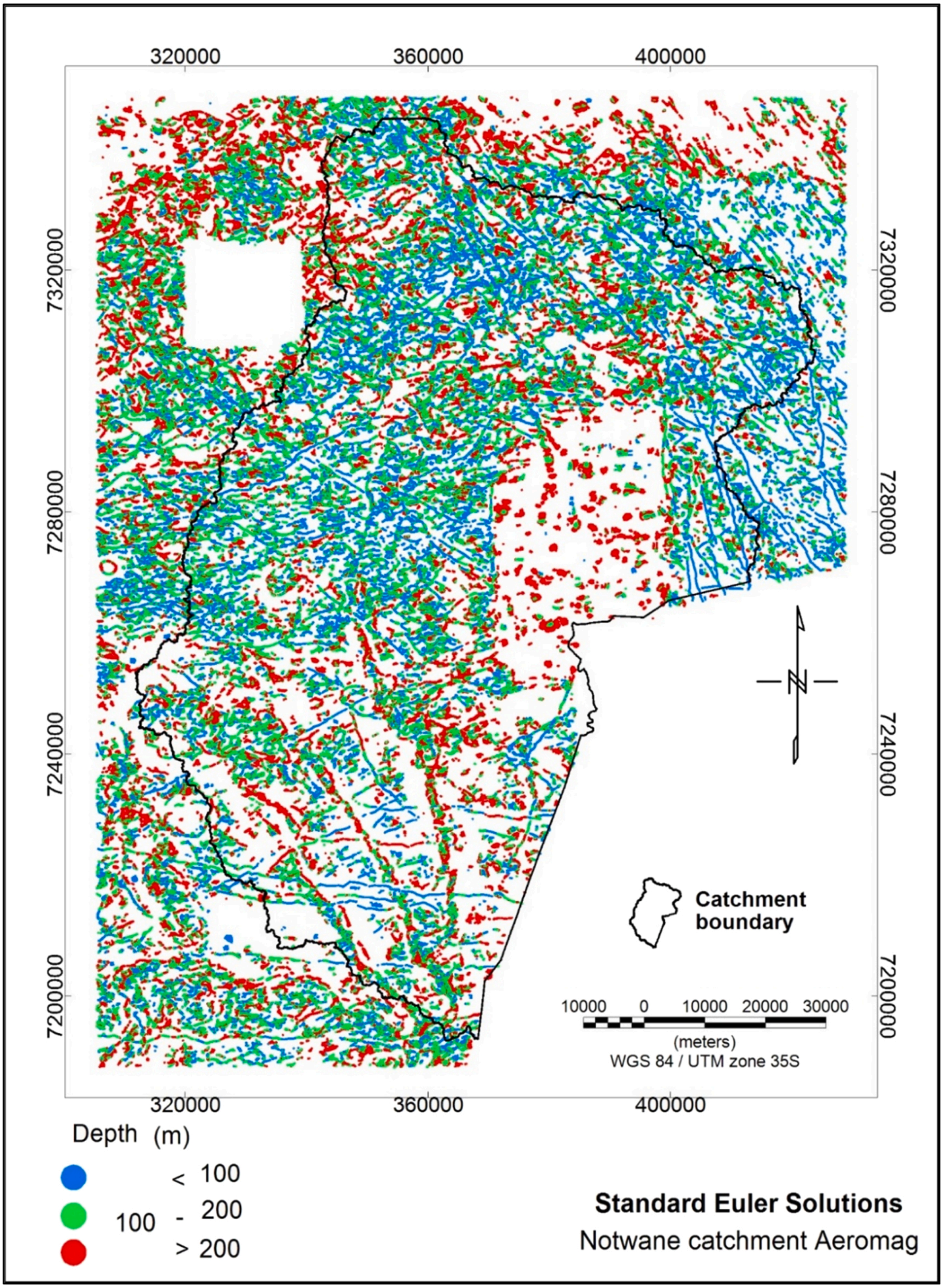

Fig. 6. Standard Euler deconvolution solutions of the study area with depth of magnetic source bodies categorized in 3 depth groups.

coincide with high subsurface and outcropping rocks of high magnetic strength. These structures are observed on the southernmost part of the study area with north-west south-east trend and also with a West East trend in the upper part of Notwane catchment.

The built-up area has expanded significantly between 2009 and 2019 resulting in an impervious land cover which has disturbed normal percolation of surface water and causing localized flooding in towns. Flooding in such areas is controlled by drainage system

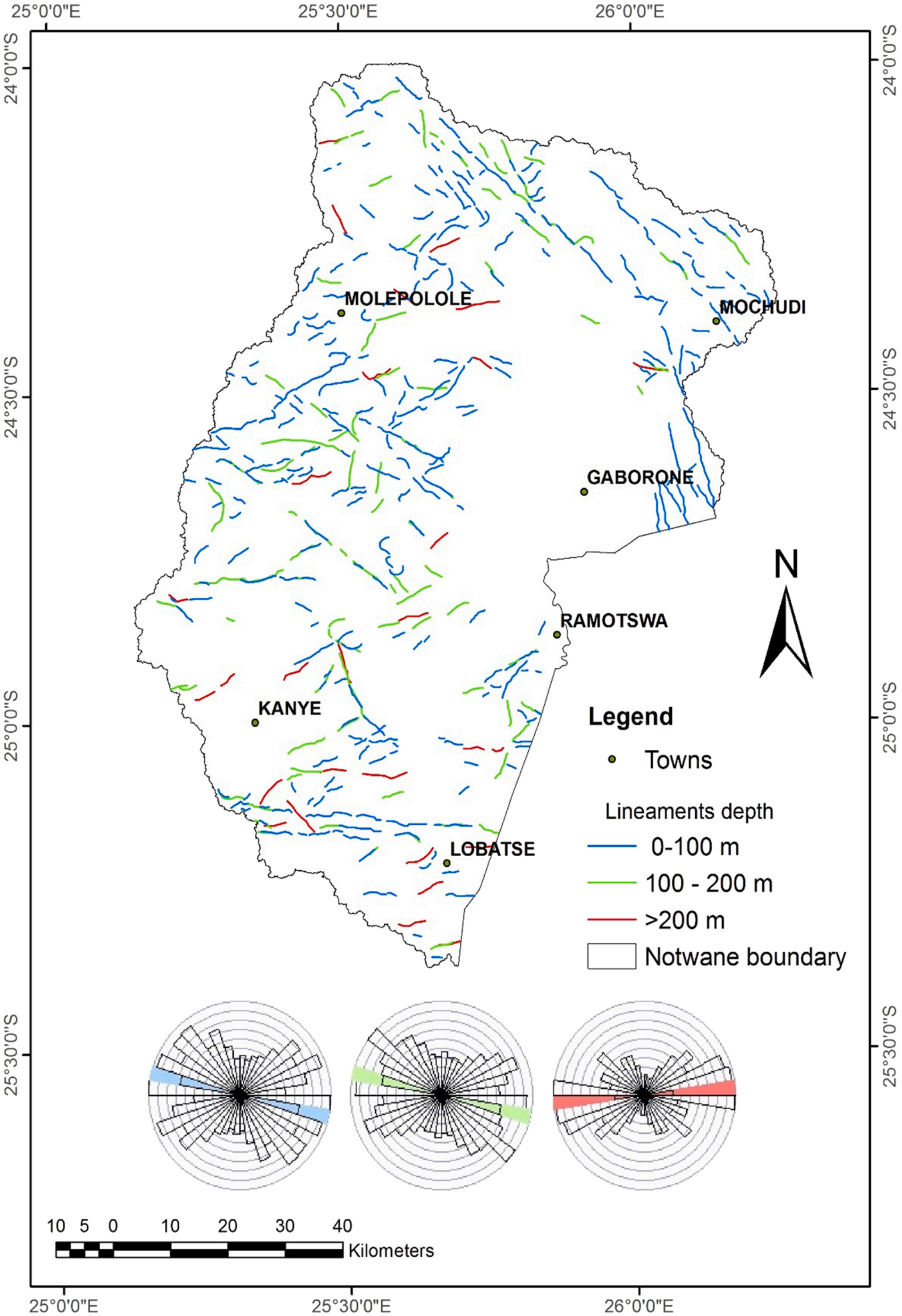

Fig. 7. Lineaments categorized in three classes of depth digitized from the standard Euler solution plots.

which drains storm water into the natural system. The amount of surface water as seen in Table 5 and Fig. 9 has reduced slightly during this period which could be attributed to abstraction to meet water demands in the area. In summary, land cover changes which did not impact the permeability of the surface are vegetation classes which only changed due to varying rainfall and other weather conditions.

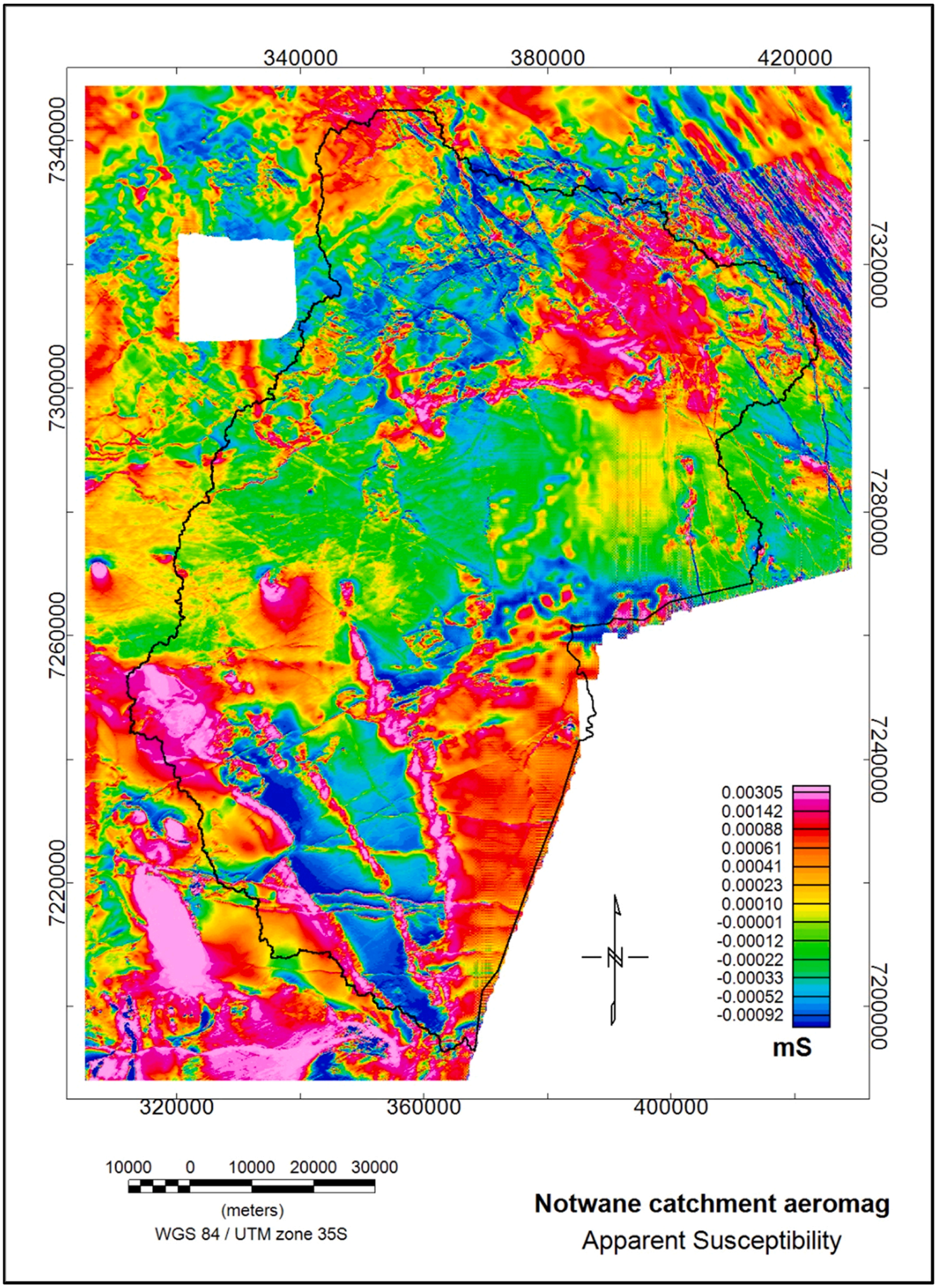

Fig. 8. Apparent susceptibility map of the study area.

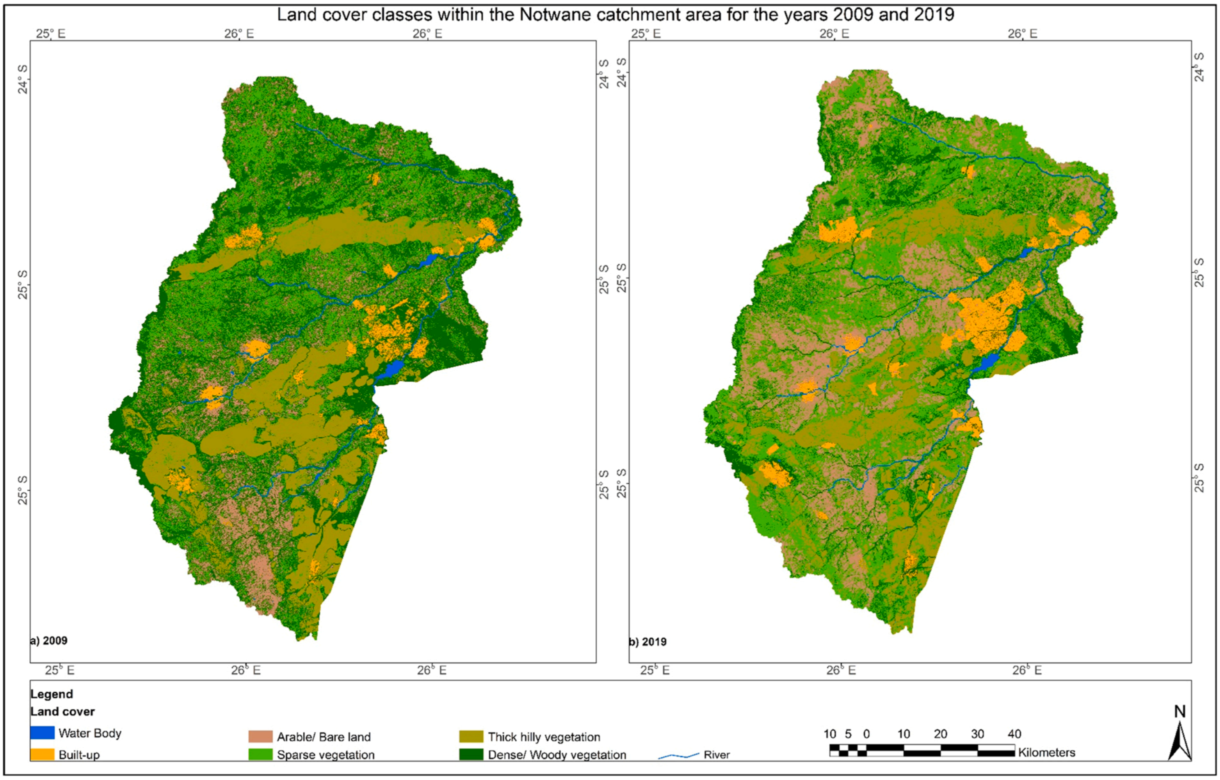

Fig. 9. Land use/ Land cover map of the Notwane catchment generated from 2009 Landsat ETM+ and 2019 Landsat 8 OLI/TIRS image.

4.2.2. DEM

The following image assortments (Fig. 10) were processed from SRTM data to generate drainage patterns for the Notwane catchment which govern the dynamics of surface runoff generated from the catchment.

The drainage system of the study area is incomplete due to administrative boundary between Botswana and South Africa and as a result limiting the study area to the Botswana side. There is a great influence of flow accumulation as some river channels flow from the neighboring country. The affected area here lies on the southeastern part of the study area along Lobatse and Ramotswa where there is a transboundary aquifer shared by the countries. The Notwane catchment area has a varying topographic relief with higher elevations bounding the area on the western side. The change in elevation is mostly gentle on the eastern side of the area which is mostly covered by ground sloping less than 2 degrees. This is suitable ground for allowing natural percolation of rainwater without discharging most of the surface as runoff.

4.3. Groundwater optimization

The following Fig. 11 is the output of the weighted overlay technique. Weights of the variables in Table 4 used in modelling potential groundwater recharge sites shown in Fig. 11 were key inputs in the AHP tool and the output was categorized in classes of four different recharge potentials being poor, minimal, moderate, and strong zones. The infeasible areas with empty output for groundwater recharge potential which have not been categorized are indicated by flow direction of surface runoff on the right map in Fig. 11 below. These are areas dominated by impervious surfaces (built-up area), steep slopes, soils with higher clay content (High FSMC) and higher apparent susceptibilities. These impervious and semi-impervious surfaces generate runoffs and prevent infiltration of rainwater which is collected through storm water drainage system which are sometimes overloaded causing floods, thus providing source of water to recharge groundwater sources.

Geological lineaments outside the built-up areas are fundamental structures that affect groundwater movement as they are conduits to groundwater flow which leads to aquifers. The slope and topography of the area affect direction of surface water flow by gravity and careful assessment of the area including the type of lithology play a vital role in determining the suitable areas that can be proposed to be ideal groundwater recharge zones.

The catchment has a total of 20 watersheds in which four are shared between Botswana and South Africa as shown in Fig. 11.

Groundwater recharge optimization draws individual aspects discussed in the methodology into an ideal recharge system where excess surface runoff generated from surplus water (flooding) is stored underground to be used during water shortage. Based on findings from a research conducted by Tafila (2020) on the Notwane catchment, there is evident trend of declining groundwater levels across the whole catchment. On the same study, runoffs were seen to have increased significantly between the years 2009 and 2019,

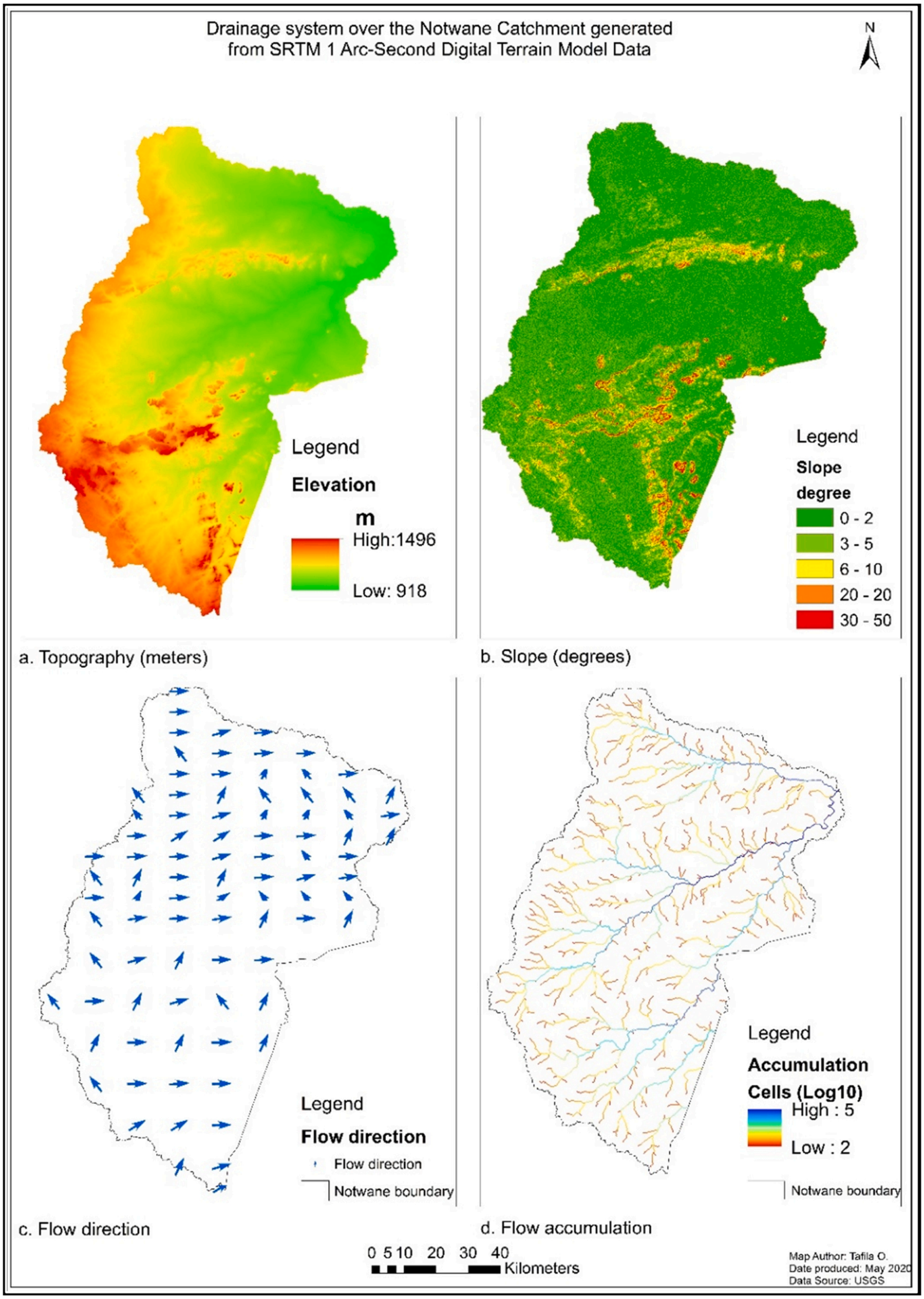

Fig. 10. Drainage system over the Notwane catchment including elevation, slope flow direction and flow accumulation.

Table 5
Summary for land cover change between 2009 and 2019.

Class Name	2009 Area (km^2)	2009 % of total area	2019 Area (km^2)	2019 % of total area	% change from 2009 to 2019
Dense/ Woody vegetation	3837.21	41.44	1527.25	16.49	-24.94
Sparse vegetation	2407.40	26.00	4022.55	43.44	17.44
Arable/ Bare land	1014.62	10.96	2063.59	22.28	11.33
Built-up	217.16	2.34	289.11	3.12	0.78
Thick hilly vegetation	1757.65	18.98	1338.12	14.45	-4.53
Water body	26.57	0.29	20.22	0.22	-0.07
Total	**9260.61**		**9260.84**		

Table 6
Confusion matrix and overall accuracy assessment summary for Landsat 8 OLI/ TIRS Land cover/ Land Use 2019 map.

CLASS		Reference data: Water Body	Dense/ Woody vegetation	Sparse vegetation	Hills With thick shrubs	Built-up (Town / Village)	Arable Land and bare ground	Reference totals	Producers accuracy %	Users accuracy %
Classified Data	Water Body	34						40	85.00	100.00
	Dense/ Woody vegetation	5	30	2	2	10		40	75.00	61.22
	Sparse vegetation		7	18	1	1	5	38	47.37	56.25
	Hills With thick shrubs	1	3		37			40	92.50	90.24
	Built-up (Town / Village)					18		40	45.00	100.00
	Arable Land and bare ground			18		11	37	42	88.10	56.06
	Column total	40	40	38	40	40	42	240		
	Overall Classification Accuracy =		72.50%							
	Overall Kappa Statistics =		0.6695							

despite the modelled runoff only considering contribution of climatic variables to the exclusion of land cover and land use changes.

Investigation of surface and subsurface of the catchment yielded input data for groundwater optimization model. The use of continuous and discrete raster datasets yielded output of different categories of recharge potential. The main strengths of the model were on variables with more influence in groundwater dynamics and these included spatial extents with high lineament densities and low apparent susceptibilities which are indicative of secondary porosities. In a similar study, Chuma and Hlatywayo (2013) has indicated that zones of increased porosity and permeability were proximal to lineaments which greatly increases the chance of groundwater accumulation. Empty output is an infeasible site due to unfavorable land use e.g., built up or rather a complex nature of the subsurface which has little relevance to groundwater sources like areas with high magnetic susceptibilities shown in Fig. 8.

Areas with higher recharge potential lies on the central part of the catchment, northeastern margin and the southernmost part bounded by topographical relief of hills with thick vegetation. The unclassified areas on the model output mainly comprise of built-up areas and areas with high magnetic susceptibilities. These areas are likely to generate increased runoff due to limited infiltration of storm water which will be redirected to watershed outlet points through areas of high flow accumulation and ultimately main river systems.

5. Conclusion

Significant geological lineaments and land covers of the Notwane catchment were generated and analyzed for potential groundwater recharge. Most lineaments generated were shallower with general East West direction whilst a few were more than 200 m deep. These lineaments combined with complex land cover of pervious and impervious surfaces provide limited potential conduits of groundwater flow within the catchment. The varied groundwater potential within the Notwane catchment is due to non-uniform distribution of theses lineaments and varied magnetic susceptibilities which are measures of intensity of weathering. It can be inferred that poor groundwater recharge potential areas are furthest from lineaments and low magnetic susceptibility zones. Areas with low elevations and high flow accumulation are potential sites for capturing runoff in detention ponds and check dams at suitable

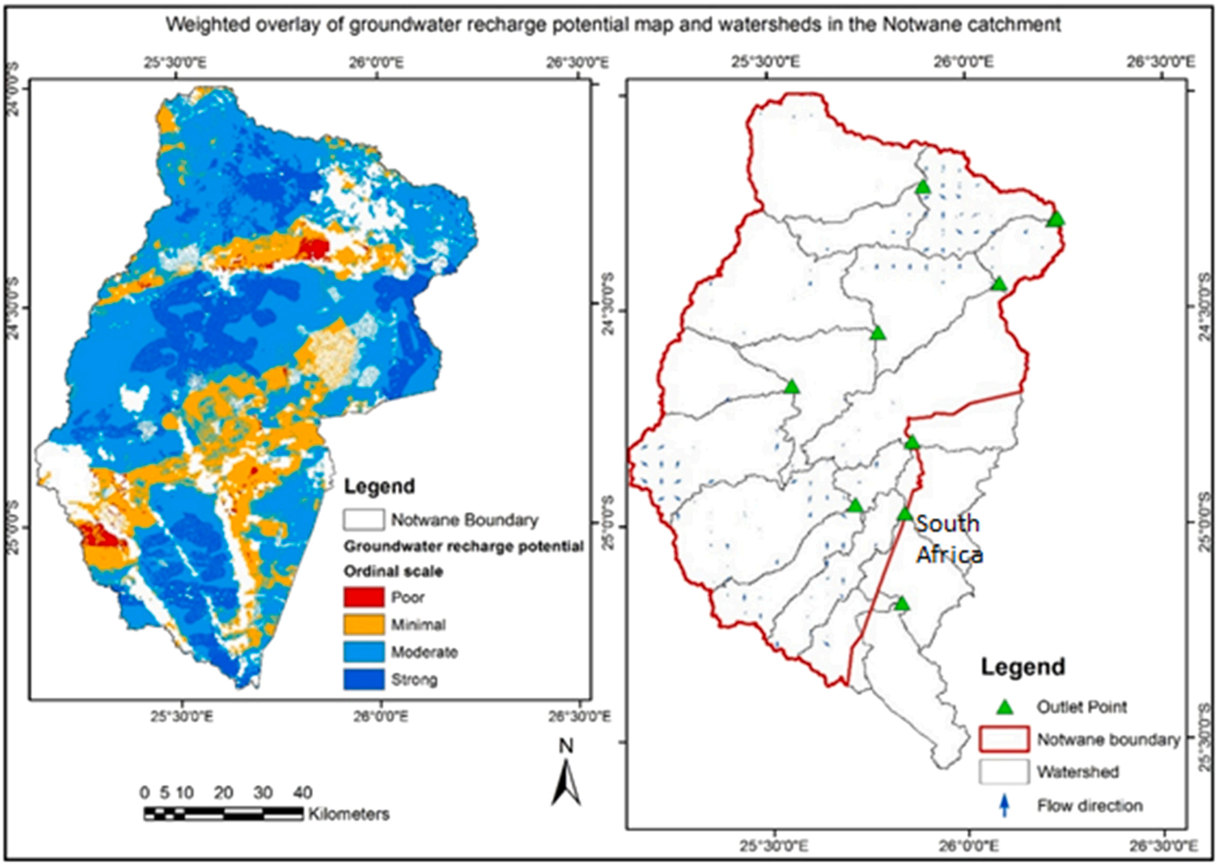

Fig. 11. Potential groundwater recharge categories in the NCA. Infeasible areas with little to no groundwater recharge potential generated empty output as notable from the map on the left. These areas are represented with flow direction of surface water on the watersheds map on the left.

watershed outlet points while areas with high elevations are less weathered and do not allow surface water to percolate without flowing to low flat area. The magnetic susceptibility map indicates that areas with high elevation have relatively high magnetic susceptibility. High magnetic susceptibility zones are presumably less weathered and lack secondary porosity for effortless groundwater recharge. Groundwater recharge optimization encompassing AHP shows that areas with higher recharge potential lie on the central part of the NCA, northeastern margin and the southernmost part bounded by topographical relief of hills with thick vegetation. Though not tested by ground follow-up methods, the multi-disciplinary approach used could offer a more reliable way to identify potential recharge zones, particularly in semi-arid hard rock terrains.

Funding

This work was supported by the Southern African Science Service Center for Climate Change and Adaptive Land Management (SASSCAL Namibia),(Botswana node), Task 303 (2015-2023).

CRediT authorship contribution statement

O. Tafila: Conceived the initial idea, did most of the data analysis, interpretations and lead in writing the manuscript. **R.T. Ranganai**: Contributed significantly to analyzing aeromagnetic data and geological background of the study area in relation to groundwater prospects and shaping the manuscript write-up. **D.B. Moalafhi**: Contributed significantly to the initial stages of the research project logistics, assisting in operationalizing key aspects of data analysis, helped in interpretations of the results of analysis and shaping the manuscript write-up. **K.K. Moreri**: Contributed significantly to the write-up by giving highly useful feedback to the draft. **J.G. Maphanyane**: Facilitated and processed funding acquisition from SASSCAL and guided in classification and interpretation of remotely sensed data used in the study.

Declaration of Competing Interest

The authors declare that they have no known competing financial interests or personal relationships that could have appeared to influence the work reported in this paper.

Acknowledgements

The authors would like to thank the Southern African Science Service Center for Climate Change and Adaptive Land Management (SASSCAL) for awarding Mr. Tafila who is the first author, a scholarship for Master of Science in Environmental Science (Geospatial Science) which lead to the development of this manuscript. We would like to acknowledge Botswana Geoscience Institute for providing archive aeromagnetic data and the United States Geological Survey (USGS) for access to satellite images used for this study. The Authors are moreover duty bound to recognize the University of Botswana for ethical clearance and support in this research.

References

Botha, F.S., Van Rooy, J.L., 2001. Affordable water resource development in the northern province, South Africa. J. Afr. Earth Sci. 33 (3), 687–692. https://doi.org/10.1016/S0899-5362(01)00093-8.
Chanda, R., Mosetlhi, B.T., Sakuringwa, S., Makwati, M., 2018. Water for Urban Development or Rural Livelihoods: is that the question for Botswana's Notwane River Catchment? Botsw. Notes Rec. 50.
Chuma, C., Dumisani, J., Hlatywayo, D., Midzi, V. , 2020. Spatial Analysis of the Structural Lineaments and Tectonics of Bulawayo Area in Zimbabwe with Repercussions for Hydrogeological Characteristics of the Crystalline Basement Aquifers (pp. 74).
Chuma, C., Hlatywayo, D.J., 2013. Geospatial Analysis of the Aquiferous Potential Zones in the Crystalline Basement of Bulawayo Metropolitan Area, Zimbabwe. 64th International Astronautical Congress, Beijing, China.
Congalton, R.G., Green, K., 2008. Assessing the Accuracy of Remotely Sensed Data: Principles and Practices. CRC press.
da Costa, A.M., de Salis, H.H.C., Viana, J.H.M., Leal Pacheco, F.A., 2019. Groundwater recharge potential for sustainable water use in Urban Areas of the Jequitiba River Basin, Brazil. Sustainability 11 (10), 2955. https://doi.org/10.3390/su11102955.
Dentith, M., Mudge, S.T., 2014. Geophysics for the Mineral Exploration Geoscientist. Cambridge University Press.
Dijon, R., 1984. Ground-water exploration in precambrian rocks of Northern Cameroon. Ground Water Hard Rocks U. N. 171.
Farahbakhsh, E., Chandra, R., Olierook, H.K., Scalzo, R., Clark, C., Reddy, S.M., Muller, R.D., 2018. Computer vision-based framework for extracting geological lineaments from optical remote sensing data. arXiv preprint arXiv:1810.02320. doi:https://doi.org/10.1080/01431161.2019.1674462.
Gieske, A.S.M. , 1992. Dynamics of groundwater recharge: a case study in semi-arid eastern Botswana.
Grant, F., 1973. Magnetic Susceptibility Mapping: The First Years Experience. Paper Presented at the 43rd Annual International Meeting. Society of Exploration Geophysics, Mexico City, p. 1973.
Hammouri, N., Al-Amoush, H., Al-Raggad, M., Harahsheh, S., 2014. Groundwater recharge zones mapping using GIS: a case study in Southern part of Jordan Valley, Jordan. Arab. J. Geosci. 7 (7), 2815–2829. https://doi.org/10.1007/s12517-013-0995-1.
Huang, F., Zhang, Y., Zhang, D., Chen, X., 2019. Environmental groundwater depth for groundwater-dependent terrestrial ecosystems in arid/semiarid regions: a review. Int. J. Environ. Res. Public Health 16 (5), 763. https://doi.org/10.3390/ijerph16050763.
Maxwell, A. , 2018. Weighted overlay in GIS. (06 July 2020). Retrieved from ⟨https://www.youtube.com/watch?v=qyNkZ2FRLb8&t=1027s⟩.
Kumari, Nemika, Krishna, Akhouri Pramod, 2013. Geospatial techniques based assessment of groundwater recharge site suitability. Int. J. Adv. Remote Sens. GIS 2, 96–109.
Moalafhi, D., Kenabatho, P., Parida, B., Matlhodi, B., 2018. Predictability of daily precipitation using data from newly established automated weather stations over Notwane catchment in Botswana. Biodivers. Ecol. 6, 46–51.
Mu, E., Pereyra-Rojas, M., 2017. Practical Decision making using Super Decisions v3: An Introduction to the Analytic Hierarchy Process. Springer.
Ranganai, R., Ebinger, C., 2008. Aeromagnetic and Landsat TM structural interpretation for identifying regional groundwater exploration targets, south-central Zimbabwe Craton. J. Appl. Geophys. 65 (2), 73–83. https://doi.org/10.1016/j.jappgeo.2008.05.009.
Rashid, M., Lone, M.A., Ahmed, S., 2012. Integrating geospatial and ground geophysical information as guidelines for groundwater potential zones in hard rock terrains of south India. Environ. Monit. Assess. 184 (8), 4829–4839. https://doi.org/10.1007/s10661-011-2305-2.
Reford, S., Nyepetsi, M., Tshoso, G., Koketso, M., Steenkamp, B., Crous, A., 2013. Botswana's Nationwide Tie Line Survey and New Magnetic Compilation, Paper presented at the 13th SAGA Biennial Conference and Exhibition, South Africa.
Reid, A.B., Allsop, J., Granser, H., Millett, A. t, Somerton, I., 1990. Magnetic interpretation in three dimensions using Euler deconvolution. Geophysics 55 (1), 80–91. https://doi.org/10.1190/1.1442774.
Reynolds, J.M., 2011. An Introduction to Applied and Environmental Geophysics. John Wiley & Sons.
Roy, I.G., 2014. Multiscale analysis of high resolution aeromagnetic data for groundwater resource exploration in an arid region of South Australia. J. Appl. Geophys. 105, 159–168. https://doi.org/10.1016/j.jappgeo.2014.03.011.
Saaty, T.L., Vargas, L.G., 2012. Models, Methods, Concepts & Applications of the Analytic Hierarchy Process, vol. 175. Springer Science & Business Media.
Saraf, A., Choudhury, P., Roy, B., Sarma, B., Vijay, S., Choudhury, S., 2004. GIS based surface hydrological modelling in identification of groundwater recharge zones. Int. J. Remote Sens. 25 (24), 5759–5770. https://doi.org/10.1080/0143116042000274096.
Silva, J.B., Hohmann, G.W., 1984. Airborne magnetic susceptibility mapping. Explor. Geophys. 15 (1), 1–13.
Tafila, O., 2020. Use of Geospatial and Geophysical Techniques to Investigate Groundwater Recharge Potential for Notwane Catchment, Botswana (Master of Science Thesis). University of Botswana.
Takorabt, M., Toubal, A.C., Haddoum, H., Zerrouk, S., 2018. Determining the role of lineaments in underground hydrodynamics using Landsat 7 ETM+ data, case of the Chott El Gharbi Basin (western Algeria). Arab. J. Geosci. 11 (4), 76. https://doi.org/10.1007/s12517-018-3412-y.
Yeh, H.-F., Cheng, Y.-S., Lin, H.-I., Lee, C.-H., 2016. Mapping groundwater recharge potential zone using a GIS approach in Hualian River, Taiwan. Sustain. Environ. Res. 26 (1), 33–43.
Yunsheng, S., Strangway, D., Urquhart, W., 1985. Geological interpretation of a high-resolution aeromagnetic survey in the Amos-Barraute area of Quebec. The Utility of Regional Gravity and Magnetic Anomaly Maps. Society of Exploration Geophysicists, pp. 413–425.
Zeil, P., Volk, P., Saradeth, S., 1991. Geophysical methods for lineament studies in groundwater exploration. A case history from SE Botswana. Geoexploration 27 (1–2), 165–177.